Science of the Total Environment 468–469 (2014) 31–45

Contents lists available at ScienceDirect

Science of the Total Environment

journal homepage: www.elsevier.com/locate/scitotenv

Integrated modelling of faecal contamination in a densely populated river–sea continuum (Scheldt River and Estuary)

Anouk de Brauwere [a,b,c,*], Olivier Gourgue [a,b], Benjamin de Brye [a,b], Pierre Servais [d], Nouho Koffi Ouattara [d], Eric Deleersnijder [a,e]

[a] Université catholique de Louvain, Institute of Mechanics, Materials and Civil Engineering (IMMC), 4 Avenue G. Lemaître, Bte L4.05.02, B-1348 Louvain-la-Neuve, Belgium
[b] Université catholique de Louvain, Georges Lemaître Centre for Earth and Climate Research (TECLIM), Chemin du Cyclotron 2, B-1348 Louvain-la-Neuve, Belgium
[c] Vrije Universiteit Brussel, Analytical and Environmental Chemistry, Pleinlaan 2, B-1050 Brussels, Belgium
[d] Université Libre de Bruxelles, Ecologies des Systèmes Aquatiques, Campus de la Plaine, CP 221, B-1050 Brussels, Belgium
[e] Université catholique de Louvain, Earth and Life Institute (ELI), Georges Lemaître Centre for Earth and Climate Research (TECLIM), Chemin du Cyclotron 2, B-1348 Louvain-la-Neuve, Belgium

HIGHLIGHTS

- *E. coli* concentrations are modelled in the whole Scheldt catchment.
- Catchment model is coupled to hydrodynamic model (tidal river and estuary).
- Results compare well to field data and model sensitivity is assessed.
- The impact of 2 wastewater management scenarios was traced down to the North Sea.
- The estuary acts as a cleaning filter removing most *E. coli* before they reach the sea.

ARTICLE INFO

Article history:
Received 8 May 2013
Received in revised form 17 July 2013
Accepted 6 August 2013
Available online xxxx

Editor: Christian EW Steinberg

Keywords:
Microbiological water quality
Escherichia coli
Modelling
Tidal rivers
Scheldt Estuary
SLIM

ABSTRACT

In order to simulate the long-term (months–years) median *Escherichia coli* distributions and variations in the tidal Scheldt River and Estuary, a dedicated module was developed for the Second-generation Louvain-la-Neuve Ice-ocean Model (SLIM, www.climate.be/slim). The resulting model (SLIM-EC2) presents two specific and new features compared to the older SLIM-EC model version. The first is that the *E. coli* concentrations in the river are split in three fractions: the free *E. coli* in the water column, the ones attached to suspended solids and those present in the bottom sediments, each with their own transport, decay and settling–resuspension dynamics. The bacteria attached to particles can settle and survive on the bottom, where they can be brought back in the water column during resuspension events. The second new feature of the model is that it is coupled to the catchment model SENEQUE-EC, which thus provides upstream boundary conditions to SLIM-EC2. The result is an integrated and multi-scale model of the whole Scheldt drainage network from its source down to the Belgian/Dutch coastal zone. This new model reproduces the long-term median *E. coli* concentration along the Scheldt River and Estuary. An extensive sensitivity study is performed demonstrating the relative robustness of the model with respect to the chosen parameterisations. In addition to reproducing the observed *E. coli* concentrations in 2007–2008 at various stations, two extreme wastewater management scenarios were considered. Overall, there is no doubt that the Scheldt Estuary acts as a cleaning filter of faecal contamination originating from large Belgian cities. As a result, at the mouth of the Scheldt Estuary *E. coli* concentration is negligible in all investigated conditions.

1. Introduction

In the framework of the Belgian Interuniversity Attraction Pole (IAP) TIMOTHY project two models were developed to describe the microbiological quality of the surface waters in the Scheldt watershed. The aims of the project are related to assessing the long-term impact of anthropogenic activities in the watershed. To achieve these aims, the preferred strategy was to combine models with field measurements. A large body of literature exists on real-time modelling of microbiological water quality using black-box, statistical models (e.g. Heberger et al., 2008 and references therein; Stidson et al., 2011). These models can be very accurate for the (short-term) prediction of water quality, but they hardly offer any mechanistic insights in the system. However, as the TIMOTHY project aimed at an integrated understanding of the driving processes and an assessment of different future scenarios, it was

* Corresponding author at: Université catholique de Louvain, Institute of Mechanics, Materials and Civil Engineering (IMMC), 4 Avenue G. Lemaître, Bte L4.05.02, B-1348 Louvain-la-Neuve, Belgium. Tel.: +32 10 47 80 26; fax: +32 10 47 21 80.
E-mail address: anouk.debrauwere@uclouvain.be (A. de Brauwere).

0048-9697/$ – see front matter © 2013 Elsevier B.V. All rights reserved.
http://dx.doi.org/10.1016/j.scitotenv.2013.08.019

decided to develop mechanistic models, modelling (as explicitly as possible) the main processes influencing the microbiological water quality in the Scheldt.

Both microbiological water quality models developed for the Scheldt consider *Escherichia coli* (*E. coli*) concentrations, as an indicator for the microbiological water quality. The two models are conceptually different, because they were originally designed for distinct types of applications. The first model (SENEQUE-EC, Ouattara et al., 2013) is a catchment model, covering all rivers and streams in the Scheldt catchment, and including detailed information on land use and wastewater outfalls. It consists of a microbiological module (having *E. coli* concentration as state variable) appended to the hydro-ecological SENEQUE/RIVERSTRAHLER model describing the functioning of rivers of large drainage network (Ruelland et al., 2007; Thieu et al., 2009). It is integrated in a user-friendly GIS-based interface and is capable of making long-term simulations on a personal computer to assess changes over years or decades. On the other hand, its representation of the water flow dynamics is simplified and with its time step of ten days, it cannot reproduce the impact of tides or extreme events. The SENEQUE-EC model is presented in detail in a separate article (Ouattara et al., 2013).

The second model (SLIM-EC2) is the chief subject of the current article. It is based on the model SLIM (Second-generation Louvain-la-Neuve Ice-ocean Model, www.climate.be/slim), whose hydrodynamic module is able to accurately resolve the tides (de Brye et al., 2010), extreme discharge events or storm surges with a 15 min time step. SLIM exists in a 1D (section-averaged) and 2D (vertically averaged) version (the 3D version is currently being developed, cf. Kärnä et al. (2013)), and both can be fully coupled on-line. This is a complex model requiring high-performance computing facilities to simulate periods that rarely exceed a few years for a limited number of state variables.

Instead of using these two tools as competing models, each of them is used in the domain for which it was originally designed and clearly outperforms the other model. SENEQUE-EC is applied to the whole Scheldt drainage network, from the source to the tidal limit (Ouattara et al., 2013), while SLIM-EC2 covers the tidal rivers, the estuary and the North Sea. In the current study, we further integrate the two models, by using the SENEQUE-EC outputs as upstream boundary conditions for SLIM-EC2. This results in an effective off-line coupling of both models, allowing a unique coverage of the whole Scheldt land–sea continuum from the source all the way to the North Sea. As such, SENEQUE-EC produces the necessary upstream boundary conditions for SLIM-EC2. Although SENEQUE-EC's timestep of 10 days does not provide information about the short-term variations, it is still much more resolved than the available datasets. It is the first time such an integrated modelling of the faecal contamination in a large catchment (more than 22,000 km^2) has been achieved. To the best of our knowledge, there is only one previous study coupling a hydrological catchment model (SWAT) to a 2D hydrodynamic model for an estuary and it considered a much smaller catchment of 113 km^2 (Bougeard et al., 2011).

The period of interest for our study on microbiological water quality in the Scheldt basin is 2007–2008, because in this period (March 2007–June 2008) a monthly monitoring was carried out at 12 sites across the basin (Ouattara et al., 2011). The performance of the two models (SENEQUE-EC for the upstream part and SLIM-EC2 for the downstream part) to represent the "real" situation will thus be mainly validated by comparison with these field measurements. Due to the monthly data interval and the very large and complex domain, the coupled model is not intended for short-term studies, e.g. one particular day. Instead, the focus lays on correctly representing the median concentration and the variability over longer periods of time, e.g. a year. An additional advantage of the coupling is that now scenarios can be assessed more accurately for the whole river–sea continuum. Changes in wastewater or land use management can be simulated in SENEQUE-EC and the effect can be traced through the tidal rivers, the estuary and even the coastal zone, if necessary, by SLIM-EC2. To illustrate this, two scenarios will be analysed in this study, in addition to the reference situation.

The objectives of this study are to

(i) refine a previous model version (SLIM-EC, de Brauwere et al., 2011b) by explicitly representing free and attached bacteria, and the link of the latter with suspended sediment dynamics;
(ii) couple the new model SLIM-EC2 with SENEQUE-EC as a "proof of concept" that modelling *E. coli* concentrations in a whole catchment–sea continuum is possible;
(iii) apply the coupled model to reproduce the current situation and assess the integrated impact of two wastewater management scenarios, as an illustration of the applicability of such an integrated model.

Although the current work is specific to the Scheldt catchment–sea continuum, we made an effort to present and discuss the model choices against a general background of the current state-of-the art models. The new SLIM-EC2 model is presented in detail in Section 2, including its coupling to SENEQUE-EC. The validation data set is described in Section 3. In Section 4 the model results are shown and discussed. First, the reference simulation results are shown and compared to the available data (Section 4.1), followed by an in-depth discussion of the model sensitivity to the different choices of its set-up (Section 4.2). Finally, SLIM-EC2 being coupled to SENEQUE-EC, we traced the impact of the two upstream wastewater management scenarios further downstream across the tidal rivers, the estuary and finally the North Sea (Section 4.3).

2. Model description

The SLIM-EC2 model is a refinement of a previous model version, SLIM-EC (de Brauwere et al., 2011b). Both models are based on the hydrodynamic model SLIM. It solves the governing equations on unstructured meshes using the discontinuous Galerkin finite element method. It is a generic model code which has already been applied to several multi-scale study domains (Gourgue et al., 2007; Lambrechts et al., 2008; de Brye et al., 2011). The new SLIM-EC2 model uses the same domain, mesh, hydrodynamics and salinity modules as the previous model version. However, the two main differences are that:

(1) SLIM-EC received constant upstream *E. coli* concentrations, while it is well known that the *E. coli* concentrations vary in time and space. In addition, de Brauwere et al. (2011a, 2011b) noticed that the *E. coli* concentrations in the tidal domain were highly dependent on the (mean) contamination levels coming from upstream. However, field data at the model boundaries are lacking to impose sensibly varying concentrations at these boundaries. Therefore, a major improvement of SLIM-EC2 is its coupling to SENEQUE-EC: the latter model now provides the upstream concentrations to the former model at 10 day-intervals.
(2) SLIM-EC only considered one type of waterborne *E. coli* (gradually disappearing due to mortality and settling), without explicit interaction with suspended particles. However, it is known that faecal bacteria can be in the water column either as free floating bacteria or attached to suspended particles (Pachepsky and Shelton, 2011). The free and attached bacteria are transported differently; in particular, the attached bacteria are subject to vertical processes (deposition and resuspension) while these processes are negligible for free bacteria. Indeed, Garcia-Armisen and Servais (2009) have shown that free *E. coli* were not subject to settling. They are also reported to be subject to different mortality rates due to the "sheltering" effect of the particles. In SLIM-EC2 (as well as in the SENEQUE-EC model) an attempt is made to take this into account.

In the following sections, the SLIM-EC2 model set-up is presented in detail.

2.1. Domain and mesh

The domain of interest for this study is the tidal Scheldt River and Estuary (Fig. 1b). The tidal Scheldt River has widths ranging approximately between 50 and 100 m and water depths of generally less than 10 m. We define the Scheldt Estuary as that part where salinity is >0; this corresponds to the part of the domain where the Scheldt starts widening from 100 m to 8 km at the mouth. Progressively, several channels appear with water depths of 20 m or more, surrounded by large intertidal flats and marshes, resulting in large lateral variations in bathymetry and water velocities. To accurately and efficiently model this, a multi-scale unstructured computational grid has been used. Firstly, it extends far beyond the actual domain of interest: from the upstream tidal river network to the North-Western European continental shelf (Fig. 1). This computational domain and the mesh are identical to those used in de Brauwere et al. (2011a, 2011b) and Gourgue et al. (2013). Secondly, the estuary and shelf are discretised on a 2D mesh, while the tidal river network consists of 1D segments, which together form a single integrated mesh. The fact that we used a 1D–2D model to simulate *E. coli* concentrations is justified for the Scheldt, which is well-mixed by the strong tides. Therefore, vertical variations are generally negligible (Baeyens et al., 1998; Vanderborght et al., 2007; de Brye et al., 2010).

The reasons why the computational domain was extended so drastically are threefold and only related to the hydrodynamics: (1) inclusion of the shelf facilitates the simulation of wind-forced processes, such as storm surges, (2) the upstream boundary conditions are more natural to enforce at the limits of the tidal influence, and (3) more accurate data are available for tidal forcing at the shelf break and for discharge at the upstream limits of the tidal influence. Although this domain extension is huge compared to the domain of interest (i.e. the Scheldt and adjacent coastal zone), still approximately 50% of the grid cells lie in the domain of interest. This is the main merit of the unstructured mesh used, whose resolution could be greatly varied in space (Fig. 1). Unstructured meshes can only be used with finite volume or finite element models. So far studies using this kind of models are still minoritary in the scientific literature on microbiological water quality (Liu et al., 2006; Schnauder et al., 2007; Bedri et al., 2011; de Brauwere et al.,

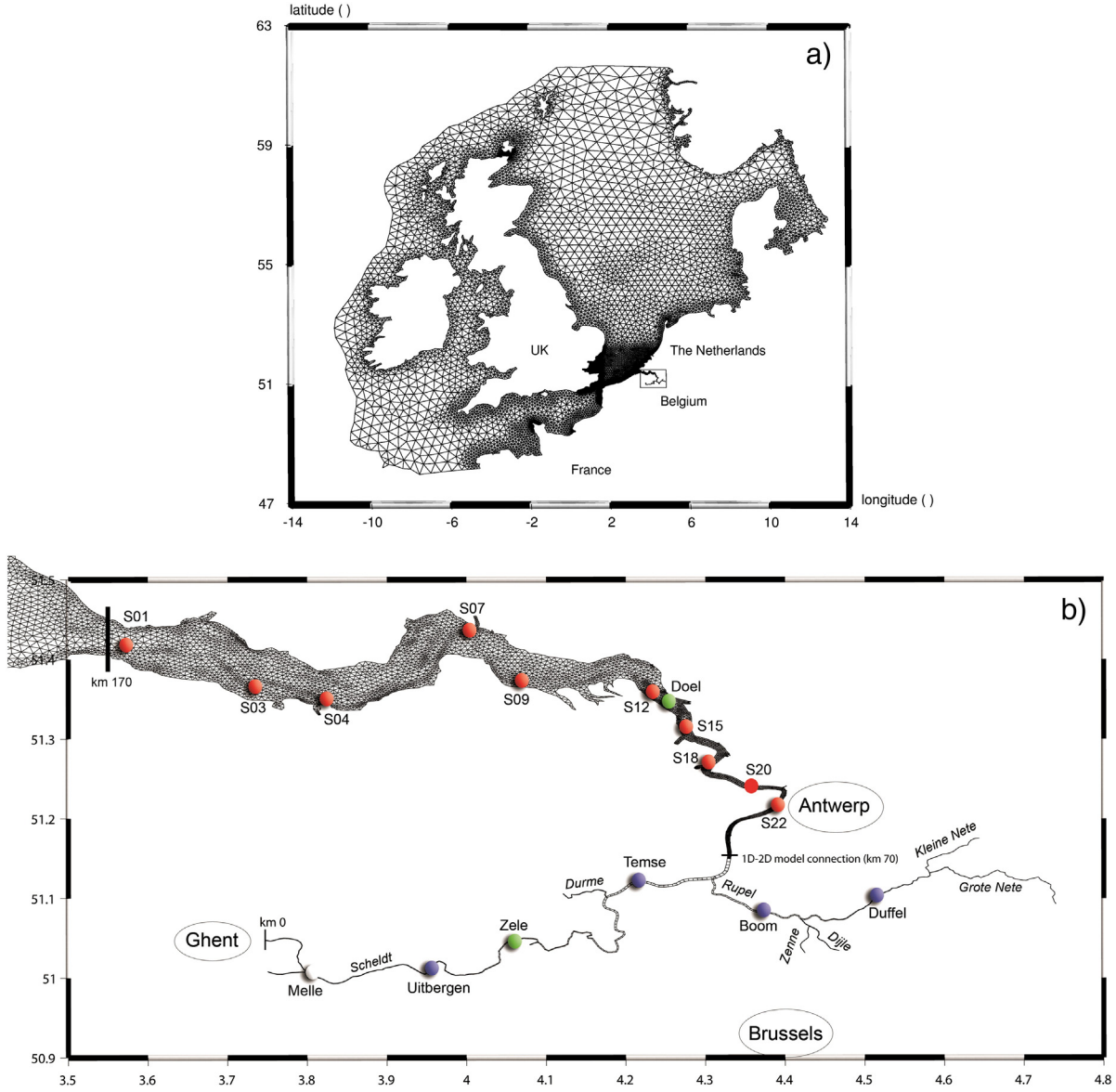

Fig. 1. Model domain and grid, showing the area of interest (Scheldt River and Estuary) covering only a small fraction of the total area, but containing a significant number of grid cells. (a) Complete mesh; (b) zoom on estuary and tidal rivers, also showing the connection between the 1D and 2D models, the different tributaries modelled as well as a few important locations (important cities are encircled, dots indicate sampling stations). km indications refer to the longitudinal axis along the Scheldt used for visualising the simulations.

2011b; Rodrigues et al., 2011; Zhu et al., 2011). The mesh size varies over several orders of magnitude: the ratio of the area of the largest triangle to that of the smallest exceeds 10^4. The smallest triangles with a characteristic length of ~60 m are in the Scheldt Estuary. The 1D elements have a length of approximately 400 m. The total mesh counts approximately 22,000 triangles (2D part) and 350 segments (1D part).

2.2. Hydrodynamics and salinity

Details on how SLIM computes the hydrodynamics (water elevation and depth-averaged velocities) and generic tracer transport can be found in de Brye et al. (2010). The setup is almost identical to the hydrodynamics used in de Brauwere et al. (2011a, 2011b). Slight changes are related to a further optimised bottom friction and diffusion applied through the 1D–2D model connection (de Brye, 2011). It is important to realise that the tide is a major dynamical feature in the whole domain studied, and the hydrodynamics was validated to represent these dynamics accurately. Time steps of 15 min ensure sufficient resolution for the tidal oscillations and can cope with sudden changes in case of extreme events. The tides are forced at the shelf break boundary; at the river boundaries measured daily discharge values are imposed. These river discharges vary significantly over the course of a year, but e.g. the average daily discharge at the Scheldt upstream boundary is approximately 40 $m^3\ s^{-1}$. The other rivers' discharges are smaller.

For the sake of simplicity only the 2D equations are presented here. The hydrodynamic variables are the water elevation η [m], and the depth-averaged horizontal velocity vector $\boldsymbol{u}$ [$m\ s^{-1}$]. The evolution is governed by the so-called shallow water equations:

$$\frac{\partial \eta}{\partial t} + \nabla\cdot(H\boldsymbol{u}) = 0, \tag{1}$$

$$\frac{\partial \boldsymbol{u}}{\partial t} + \boldsymbol{u}\cdot(\nabla\boldsymbol{u}) + f\boldsymbol{k}\times\boldsymbol{u} = -g\nabla\eta - \frac{1}{\rho}\nabla p_a + \frac{1}{H}\nabla\cdot(H\nu(\nabla\boldsymbol{u})) + \frac{\boldsymbol{\tau}_s - \boldsymbol{\tau}_b}{\rho H}, \tag{2}$$

where t is the time, ∇ is the del operator, $H = h + \eta$ is the total water depth, with h the reference height of the water column, $f = 2\omega \sin\phi$ is the Coriolis parameter, with ω the angular velocity of the Earth and ϕ the latitude, $\boldsymbol{k}$ is the unit upward vector, g is the gravitational acceleration, ρ is the water density which is assumed to be constant, in accordance with the Boussinesq approximation, p_a is the atmospheric pressure at the water surface, ν is the horizontal eddy viscosity, $\boldsymbol{\tau}_s$ and $\boldsymbol{\tau}_b$ are the surface and bottom stress vectors, respectively. The bottom stress vector is parameterised using the Chézy–Manning–Strickler formulation:

$$\boldsymbol{\tau}_b = \rho g n^2 \frac{\boldsymbol{u}\|\boldsymbol{u}\|}{H^{1/3}}, \tag{3}$$

where n is the Manning coefficient, depending on the physical properties of the bottom. Its value is calibrated to represent the tide correctly. It is equal to 0.0235 $s\cdot m^{-1/3}$ on the continental shelf and increases linearly from the mouth to a value 0.028 $s\cdot m^{-1/3}$ around Antwerp (de Brye et al., 2010).

The depth-averaged salinity S [–] obeys the following transport equation:

$$\frac{\partial}{\partial t}(HS) + \nabla\cdot(\boldsymbol{HuS}) = \nabla\cdot(H\kappa\nabla S). \tag{4}$$

The diffusivity κ is parameterised by Okubo's formulation (Okubo, 1971):

$$\kappa = c_\kappa \Delta^{1.15}, \tag{5}$$

where c_κ is a constant and Δ is the characteristic local length scale of the mesh (i.e. the longest edge of a triangle in the 2D part, or the segment length in the 1D part). Its value of 150 $m^{0.85}\ s^{-1}$ has been calibrated to accurately represent the salinity variations in the Scheldt (de Brye et al., 2010).

For more information on calibration, validation and numerical details of the hydrodynamics and salinity modules, we refer to de Brye et al. (2010).

2.3. Suspended and bottom sediment dynamics

A sediment module is added to SLIM to simulate the suspended solids and bottom sediment concentrations. The module is described and validated in detail in Gourgue et al. (2013). The module considers only one type of cohesive sediments, but describes their fate in three conceptual compartments or phases:

(1) The suspended solids (SS) in the water column (with concentration C_{SS} [$kg\ m^{-3}$]) are transported horizontally by advection and diffusion, as a dissolved tracer. In addition, they are also subject to vertical processes, locally increasing (by resuspension) or decreasing (by deposition) C_{SS}.
(2) When the particles in suspension settle to the bottom they become part of the freshly deposited layer (concentration C_{sb} [$kg\ m^{-2}$]). This layer is not transported horizontally. C_{sb} locally increases by deposition and decreases due to resuspension.
(3) Below the layer of freshly deposited sediments, a parent layer is considered. This layer is assumed to be an infinite source of sediments. It is never supplied: settling of suspended matter only forms fresh bottom sediments and there is no interaction between the two bottom layers accounting for e.g. compaction. However, if the freshly deposited layer is locally depleted and the bottom shear stress is high enough, the parent layer can be eroded. The main use of this parent layer is to accelerate the initial spin-up of the SS simulations.

These concepts are formalised in the following 2D advection–diffusion–reaction equations for C_{SS} and C_{sb} (for the sake of simplicity, only the 2D equations are presented here; for the 1D equations we refer to Gourgue et al. (2013)):

$$\frac{\partial}{\partial t}(HC_{SS}) + \nabla\cdot(H\boldsymbol{u}C_{SS}) = \nabla\cdot(H\kappa\nabla C_{SS}) + E + E_p - D, \tag{6}$$

$$\frac{\partial C_{sb}}{\partial t} = D - E \tag{7}$$

where E is the erosion rate of sediments from the freshly deposited bottom layer, E_p is the erosion rate from the parent layer and D is the deposition rate of suspended sediments to the fresh layer. Bed-load transport is not considered in the model (Gourgue et al., 2013). Deposition and resuspension rates are further parameterised as functions of salinity, temperature, C_{SS} and bottom sediment composition. The parameterisations of the erosion rates are based on a formula introduced by Partheniades (1965):

$$E_b = \begin{cases} M\left(\frac{\tau_b}{\tau_e} - 1\right) & \text{if } \tau_b > \tau_e \text{ and } C_{sb} > 0 \\ 0 & \text{otherwise} \end{cases} \tag{8}$$

$$E_p = \begin{cases} M\left(\frac{\tau_b}{\tau_e} - 1\right) & \text{if } \tau_b > \tau_e \text{ and } C_{sb} = 0 \\ 0 & \text{otherwise} \end{cases} \tag{9}$$

so that there is only erosion of sediments when the norm of the bottom stress vector τ_b exceeds a threshold value τ_e. If sediments are present in the fresh layer ($C_{sb} > 0$), this layer is eroded, otherwise sediments from the parent layer are resuspended. The erodability (τ_e) of both layers is identical. τ_e is further parameterised as a function of temperature (as a proxy for biological activity) and bottom

sediment composition (mud proportion). The first is to account for the observation that biological activity increases the cohesiveness of muddy bottom sediments, making them more difficult to erode (Stolzenbach et al., 1992; Manning et al., 2010; van der Wal et al., 2010). The second expresses that the presence of sand decreases the cohesiveness of bottom sediments (Vanoni, 2006). τ_e varies from 0.125 to 0.5 N m^{-1}. M's value is varied from 2×10^{-5} to 10^{-4} kg m^{-2} s along the estuary to account for the effect of the convergence zone of bottom currents in the area of the main estuarine turbidity maximum (Baeyens et al., 1998; Verlaan et al., 1998).

The parameterisation of the settling rate is based on a formula introduced by Einstein and Krone (1962):

$$D = w_s(C_{SS}, S, T)C_{SS} \tag{10}$$

implying that deposition occurs continuously, but with a settling velocity depending on a number of external factors. In fact, w_s is greatly influenced by flocculation, i.e. the processes by which suspended sediment particles aggregate to form larger flocs, and those flocs break up again. Large flocs are more likely to form when C_{SS} and salinity are high. In addition, biological activity has been reported to enhance floc formation and this is taken into account by a temperature dependence. The resulting formula for the settling speed is of the form $w_s = w_{s,0}(S,T)\left(\frac{C_{SS}}{C_{SS,0}}\right)^m$, where $w_{s,0}$ varies linearly with S and T, ranging from 0.25 mm s^{-1} in cold, freshwater to 5 mm s^{-1} in warm, salty water; $m = 1$ and $C_{SS,0} = 0.1$ kg m^{-3}. For more details on these parameterisations, as well as on the calibration and validation of the sediment module we refer to Gourgue et al. (2013).

The sediment transport dynamics within an estuary is intrinsically three-dimensional. Nevertheless, our approach using a depth-averaged model proved sufficiently accurate for the Scheldt Estuary, producing results rather similar to those obtained with more a complex three-dimensional model (LTVmud, van Kessel et al., 2011) in a three-month simulation comparison (Gourgue et al., 2013).

2.4. E. coli dynamics

The *E. coli* concentrations simulated by the SLIM-EC2 model represent concentrations of three types of culturable *E. coli* (Fig. 2):

(1) The free bacteria (with concentration C_f [*E. coli*·m^{-3}]) that enter the domain by external sources are subsequently transported by advection and diffusion in the water column. They are not subject to settling (Jamieson et al., 2005a; Hipsey et al., 2008; Garcia-Armisen and Servais, 2009), but they gradually die following first order kinetics. This results in the following advection–diffusion–reaction equation in 2D (all symbols are defined in Table 1):

$$\frac{\partial}{\partial t}\left(HC_f\right) + \nabla\cdot\left(H\boldsymbol{u}C_f\right) = \nabla\cdot\left(H\kappa\nabla C_f\right) + HR_f, \tag{11}$$

with R_f the source-sink terms, i.e. the decay due to mortality and the input from the sources:

$$R_f = -k_f C_f + \Sigma_f. \tag{12}$$

The 1D equations for the *E. coli* dynamics are given in Appendix A.

(2) The *E. coli* attached to the SS (with concentration $C_a C_{SS}$ [*E. coli* m^{-3}]*) are transported, settle and their stock is supplied by resuspension in the same way as the particles they are adsorbed to. In addition, they also decay, but with a different decay constant than the free bacteria (cf. Table 2):

$$\frac{\partial}{\partial t}(HC_aC_{SS}) + \nabla\cdot(H\boldsymbol{u}C_aC_{SS}) = \nabla\cdot(H\kappa\nabla(C_aC_{SS})) + HR_a, \tag{13}$$

with the source-sink terms containing resuspension (erosion), deposition, mortality and source inputs:

$$R_a = \frac{1}{H}(C_bE - C_aD) - k_aC_aC_{SS} + \Sigma_a. \tag{14}$$

(3) The bacteria attached to the freshly deposited bottom sediments (with concentration C_bC_{sb} [*E. coli* m^{-2}]) are not transported, identically to the fresh bottom sediments. Their concentration is influenced by settling of attached bacteria, resuspension, and mortality:

$$\frac{\partial}{\partial t}(C_{sb}C_b) = R_b = C_aD - C_bE - k_bC_{sb}C_b. \tag{15}$$

The characteristics of the different *E. coli* types are summarised in Table 2. There is a growing consensus in today's literature about the potential importance of bacteria on the sediment floor, and therefore the necessity to include the processes of settling and resuspension in mechanistic models of faecal contamination of surface waters (Jamieson et al., 2005b; Pachepsky and Shelton, 2011 and references therein). With this aim, most recent models indeed consider that the freely floating bacteria behave differently from those attached to particles. Nevertheless, there is no general agreement on how best to translate this knowledge

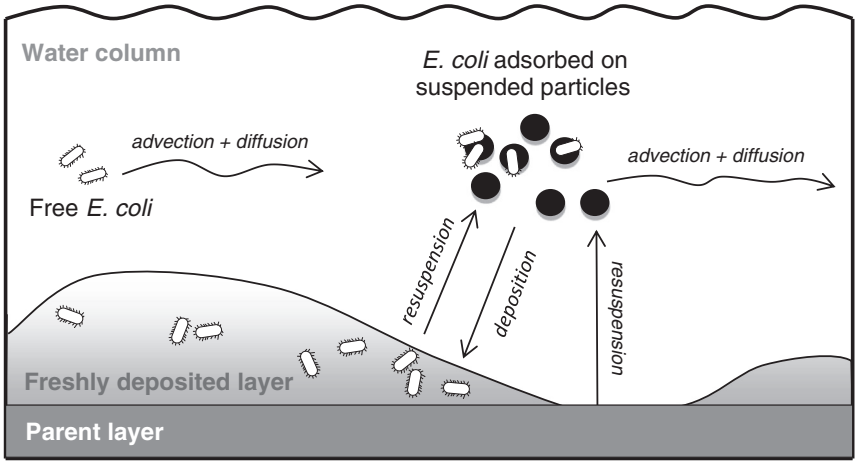

Fig. 2. Schematic representation of the three types of *E. coli* considered in SLIM-EC2, as well as the physical processes acting on them (advection, diffusion, deposition and resuspension). In addition, each type is also subject to an exponential decay with its own decay constant.

Table 1
Description and units of used symbols (only related directly to the *E. coli* dynamics).

Symbol	Units	Meaning
C_a	*E. coli* kg^{-1}	Concentration of *E. coli* attached on SS
C_b	*E. coli* kg^{-1}	Concentration of *E. coli* attached to bottom sediments
C_f	*E. coli* m^{-3}	Concentration of free floating *E. coli*
C_{sb}	kg m^{-2}	Concentration of particles on the bottom
C_{SS}	kg m^{-3}	Concentration of SS
D	kg m^{-2} s^{-1}	Deposition rate of SS (and attached *E. coli*)
E	kg m^{-2} s^{-1}	Erosion rate of bottom sediment (and bottom *E. coli*)
H	m	Water height
k_i	s^{-1}	Mortality rate constant ($i \in \{f,a,b\}$)
k_i^{20}	s^{-1}	Mortality rate constant at 20 °C ($i \in \{f,a,b\}$)
κ	m^2 s^{-1}	Diffusivity constant in the water column
T	°C	Temperature
u	m s^{-1}	Depth-averaged velocity vector
∇	m^{-1}	Del operator
Σ_i	*E. coli* m^{-3} s^{-1}	Input by the point sources (WWTPs)

into a model. We decided to explicitly divide the total pool of *E. coli* into "free" and "attached", because (i) this allows to explicitly describe their different dynamics and (ii) no assumption has to be made about the *fraction* of the total *E. coli* pool which is attached (instead, the attachment fraction is now an *output* of the model and varies in time and space). Some other recent studies still consider a single bacteria pool and either neglect settling and resuspension (Manache et al., 2007; Bedri et al., 2011; Romeiro et al., 2011; Zhu et al., 2011) or parameterised the settling term with a constant "attachment fraction" to express that settling only influences a part of the total pool (McCorquodale et al., 2004; Liu et al., 2006; Hipsey et al., 2008; Cho et al., 2010; Liu and Huang, 2012). The latter approach has the weakness to use "bacteria-specific" settling (and resuspension) fluxes which were not necessarily validated against SS data (as is done in the current study).

Once the total pool of *E. coli* is split in "free" and "attached" species, it is necessary to make an assumption about their interaction. In reality, the free-floating bacteria can adsorb on particles, and thus become "attached" bacteria; and these can again desorb to return to being "free". In order to explicitly represent these adsorption–desorption processes in the model the associated kinetics must be known. However, to the best of our knowledge, these have not been thoroughly established yet and including kinetic adsorption–desorption equations has not been attempted by any modelling study. Instead, one of the following simplifying hypotheses is generally made:

(i) Adsorption–desorption processes are fast compared to the other processes and hence an equilibrium is established at any point and time between the free and attached bacteria, quantified by an equilibrium constant (Bai and Lung, 2005; Vergeynst et al., 2010; Gao et al., 2011). Very similarly, the fraction of attached bacteria is sometimes assumed to be known (Dorner et al., 2006; Wu et al., 2009).
(ii) Attachment–detachment processes are slow compared to the other processes and thus no interaction or exchange between the free and attached bacteria is assumed (Jamieson et al., 2005a; Garcia-Armisen et al., 2006; Ouattara et al., 2013).

Table 2
Characteristics of the three types of *E. coli* considered in the SLIM-EC2 model.

	Free in water column	Attached to SS in water column	Attached, in (fresh) bottom sediment
Concentration	C_f [*E. coli* m^{-3}]	C_a [*E. coli* kg^{-1}] $C_a C_{ss}$ [*E. coli* m^{-3}]	C_b [*E. coli* kg^{-1}] $C_b C_{sb}$ [*E. coli* m^{-2}]
Source	WWTPs, proportion of total input according to treatment	WWTPs, proportion of total input according to treatment	/
Transport	Advection–diffusion	Advection–diffusion	None
Settling	No	Yes, at rate of SS	Yes, at rate of SS
Resuspension	No	Yes, at rate of SS	Yes, at rate of SS
Mortality	$k_f^{20} = 0.045\ h^{-1} = 1.25e{-}5\ s^{-1}$	$k_a^{20} = 0.0225\ h^{-1} = 6.25e{-}6\ s^{-1}$	$k_b^{20} = 0$

It is known from the general literature on bacterial adhesion onto surfaces that bacteria can, after a first reversible binding to particles by adsorption, synthesise exopolymers that strengthen their attachment to the surface (Fletcher, 1996). With such a biological binding, the fast and reversible character of the attachment is questionable (Jamieson et al., 2005a). Therefore, we preferred to use hypothesis (ii). In addition, hypothesis (i) requires an accurate knowledge of the in-situ equilibrium or attachment fraction. Based on the available data, no clear equilibrium function or fixed attachment fraction could be identified in the Scheldt. Another argument is that with hypothesis (i), the in situ attachment ratio is independent of the attachment ratio of the external sources, which limits the sensitivity of the model with respect to the sources, and hence also reduces the independent inferences that can be made from it. Conversely, with hypothesis (ii) the fraction of attached bacteria is a diagnostic variable predicted by the model which is not directly imposed as a model input. In summary, in the SLIM-EC2 model *E. coli* enter the water as either "free" or "attached", they remain this type until they die and in the mean time both types of bacteria evolve differently and independently.

Bacteria are assumed to be absent in the parent layer (i.e. the parent layer resuspension arrow in Fig. 2 does not carry any *E. coli*). This is equivalent to assuming that all bacteria that would have been present initially in the parent layer have died before they would be resuspended in the water column.

In line with the fact that the model represents concentrations of culturable *E. coli*, the "mortality" process may also include loss of culturability. This decay term lumps many effects (grazing, natural mortality, inactivation by light, etc.) and is modelled by a first order decay. This type of parameterisation is the one generally used in the broad literature on faecal bacteria modelling. It has recently been reported that decay in surface water follows a biphasic pattern, characterised by an initial faster decay rate followed by a slower die-off (Bucci et al., 2011). This has been attributed to the presence of a refractory subpopulation which is more resistant to the ambiant environment. Two modelling studies have already attempted to include this by explicitly simulating two types of bacteria, which grow/decay at a different rate (Hellweger and Masopust, 2008; Bucci et al., 2012). Again, each individual decay rate was parameterised as a first-order process, but the combination of the two is compatible with the biphasic pattern. This approach is still rather unique and most studies do not make the distinction between different subpopulations of bacteria — probably because including this in a model necessitates additional data on the composition in terms of subpopulations of the sources and boundary conditions which are unavailable. In summary, the first order decay parameterisation is a general feature in faecal bacteria models. However, the decay constants are often further refined as functions of environmental conditions (de Brauwere et al., 2013). Numerous studies reported that temperature was the main environmental factor driving mortality rate. In the temperature range usually found in surface waters a temperature increase results in an increase of the decay rate (Barcina et al., 1986; Flint, 1987; Craig et al., 2004). This can be explained by (i) a better survival at low temperature due to lower energy costs from reduced metabolic activities and (ii) higher grazing rates at high temperature due to a higher abundance of protozoa (the main bacterial grazers) and a higher grazing rate per protozoa (Servais et al., 1985; Menon et al., 2003). In our case, the mortality constants used in Eqs. (12), (14) and (15) are temperature-dependent, according to the following relationship already used in several studies (Beaudeau et al., 2001; Servais et al., 2007a, 2007b; de Brauwere et al., 2011b):

$$k_i(T) = k_i^{20}\,\frac{e^{\left(-\frac{(T-25)^2}{400}\right)}}{e^{\left(-\frac{25}{400}\right)}},\ i \in \{f,a,b\}, \tag{16}$$

with k_i^{20} the mortality constant at 20 °C and T the temperature in °C of one of the three *E. coli* types. A single temperature time series is assumed for the whole domain. The values are obtained by averaging in situ measurements at three monitoring stations in the Scheldt and at two different depths. The measurements were made at 10 min intervals and interpolated to correspond to the model time steps of 15 min. For any given moment, the measurements did not vary more than 1 °C between sites. Measurements were provided by Hydro Meteo Centrum Zeeland (www.hmcz.nl).

The mortality rate of the bacteria is different depending on the "type" they are. In general: $k_f > k_a > k_b$ (Garcia-Armisen and Servais, 2009; Pachepsky and Shelton, 2011). The k_f^{20} and k_a^{20} values used in this study (Table 2) are identical to the values used in the upstream drainage network by Ouattara et al. (2013), in order to be consistent in the whole geographical domain. The same values for k_f^{20} and k_a^{20} were also used in a previous modelling study in the Seine Estuary (Garcia-Armisen et al., 2006) and they fall within reported ranges of decay rates in other faecal bacteria modelling studies (Le Hir et al., 1990; Steets and Holden, 2003; Hipsey et al., 2008; Wu et al., 2009). In addition, the fact that the free bacteria die two times faster than the ones attached to particles is in agreement with experimental observations (Garcia-Armisen and Servais, 2009). k_b was set to zero, while it was set to a small but non-zero value ($k_b^{20} = 1.25 \times 10^{-6} s^{-1}$) in the upstream catchment (SENEQUE-EC model, cf. Ouattara et al., 2013). This has been done mainly to better fit the observations (especially the percentage of attached *E. coli* — see Section 4.2 for a more detailed discussion), but both values fall within the range of reported values, either in the experimental or modelling literature. For instance, in their extensive literature review on faecal indicator bacteria in sediments, Pachepsky and Shelton (2011) concluded that *E. coli* decay rates in sediment were highly variable but, on average, one order of magnitude lower than those in the overlying water column. On the other hand, in the only four published modelling studies we found that we have been explicitly considering bacteria in the bottom sediments, three of them imposed no decay ($k_b = 0$), as we did (Steets and Holden, 2003; Stapleton et al., 2007; Gao et al., 2011) while the fourth used a value even smaller than Ouattara et al. (2013): $k_b = 10^{-9} - 10^{-8}$ s^{-1} (Cho et al., 2010).

In contrast to some other studies, here no explicit dependence on salinity or light has been included for the decay rates. According to a collection of literature data, indeed, the general salinity dependence for the *E. coli* decay rate appears to be rather weak (cf. Fig. 5 in Hipsey et al., 2008). Generally, studies including an explicit light inactivation function investigate rather shallow and/or clear waters (streams, coastal zones) and/or areas associated with sunny climate (e.g. Connolly et al., 1999; Sanders et al., 2005; Hipsey et al., 2008; Cho et al., 2010). In a statistical regression study in five rivers in Normandy (north of France, i.e. close to our study area) Beaudeau et al. (2001) found that light was not a significant factor to predict the mortality rate. Based on these studies, we assumed that light inactivation would have a negligible effect in the Scheldt, especially due to its high turbidity (values of 500 mg L^{-1} are not unusual in the estuarine turbidity maximum zone). The case studies presented in Hipsey et al. (2008) for which the relative importance of different factors on the decay rate also seem to suggest that the temperature dependence is the most important one to consider.

2.5. E. coli sources

Ouattara et al. (2011) estimated the flux of *E. coli* emitted by both diffuse and wastewater treatment plant (WWTP) sources at the scale of the whole Scheldt watershed. According to their estimate, WWTPs release 35 times more *E. coli* than diffuse sources do. Considering, moreover, that our domain of interest is limited to the downstream, most urbanised and populated area of the watershed, it seems justified that WWTP outfalls are the only sources included in the SLIM-EC2 model (see also de Brauwere et al. (2011b)).

WWTP data are compiled from information provided by the Vlaamse Milieumaatschappij (Flemish Environmental Agency, VMM), Rijkswaterstaat Zeeland and Waterschap Zeeuwse Eilanden. Data processing steps involved the localisation of the WWTP outlet, the actual discharge point in the model domain, and the distance between these two points. The number of *E. coli* discharged by a WWTP per unit of time was approximated to be proportional to the average volume treated in the WWTP per unit of time, with a proportionality constant (*E. coli* concentration) depending on the treatment type applied in the WWTP (Ouattara et al., 2011, 2013). The *E. coli* concentrations considered in the treated effluents were 1.6×10^5 *E. coli* (100 mL)$^{-1}$ when a primary treatment was followed by an activated sludge process, 5.0×10^4 *E. coli* (100 mL)$^{-1}$ when the N removal treatment (nitrification + denitrification) was added to an activated sludge process, and 2.0×10^4 *E. coli* (100 mL)$^{-1}$ when the treatment included activated sludge followed by N and P removal; these values result from measurements performed in treated effluents of various WWTPs located in the Scheldt watershed (Ouattara et al., 2011). For all WWTPs, it was assumed that 50% of the *E. coli* in the effluent was attached to suspended solids (see Fig. 3 in Ouattara et al., 2013).

2.6. SENEQUE-EC model

The SENEQUE-EC model is used to simulate the *E. coli* concentrations in the Scheldt drainage network upstream of the tidal limit. The SENEQUE-EC model and its results are described in detail in Ouattara et al. (2013). Here we will only present the key features of the model. The model consists of a microbiological module appended to a hydro-ecological model describing the functioning of the entire Scheldt drainage network. The microbiological module describes the sources of *E. coli* (input by wastewater release but also by runoff and soil leaching), their transport and their decay once released into the natural environment. As in the SLIM-EC2 model, the dynamics of three types of *E. coli* are differentiated: free *E. coli*, *E. coli* attached to suspended solids in the water column and *E. coli* present in sediments. The SENEQUE-EC model also considers the settling of attached *E. coli* and the possible resuspension of *E. coli* deposited in the sediments. With its time step of 10 days it cannot reproduce the effect of tides or extreme events, which is why it is limited to the non-tidal rivers in the Scheldt catchment.

2.7. E. coli boundary conditions and coupling with SENEQUE-EC

At the shelf break boundaries both the *E. coli* and suspended sediment concentration are set to zero. Note that this boundary is very far from the domain of interest and from any sources of faecal bacteria. *E. coli* concentrations are not measured at this large distance from shore, but we may be confident that the waters beyond the shelf break do not act as a source of *E. coli*. No sources are considered along the adjacent Belgian and Dutch coasts either, because estuarine *E. coli* observations do not show elevated concentrations close to the mouth. It is expected that these coastal sources are quickly diluted and advected off-shore.

As explained in the Introduction, high-frequency data at the upstream boundaries would be needed in order to perfectly account for this important boundary condition in the SLIM-EC2 model. Unfortunately such measurements are not available. In this study, the upstream boundary conditions for the SLIM-EC2 model are provided by the SENEQUE-EC model. Considering that SENEQUE-EC has a 10-day time step, the boundary concentrations are still not highly resolved in time and therefore will not represent short-term extreme conditions. However, monthly and seasonal variations are well represented. The impact of the relatively slowly varying boundary conditions is assessed in more detail in Section 4.2. The coupling is off-line and only in one way. Indeed, SENEQUE-EC does not require downstream boundary conditions, as it assumes unidirectional flow. At the tidal limits of the Scheldt basin

this assumption is acceptable because the flow is either controlled by sluices or the tides are negligible. The outputs produced by SENEQUE-EC at the connection boundaries are interpolated to obtain values every 15 min — these are the actual boundary conditions for SLIM-EC2.

2.8. E. coli initial conditions and simulation period

All simulations presented in this study were started with all faecal bacteria concentrations set to zero. Once the simulation starts, the domain is progressively "filled" with *E. coli* by inputs from upstream and from the WWTPs. Attached *E. coli* can settle to the bottom. All *E. coli* simulations started on 1st February 2007, while the hydrodynamics and sediment simulations started on 1st January 2007 (so these were well established by the start of the *E. coli* simulations). Except if mentioned differently, simulation results shown in this study consider the period 26 March 2007–15 June 2008, because this period is covered by a monthly monitoring (see next section).

3. Validation data sets

The model results presented below are compared to the scarce measurements available. The main source of data comes from a monthly monitoring of several fixed sampling stations in the Scheldt drainage network performed from March 2007 to June 2008 (Ouattara et al., 2011), which is why this was the period of interest in this modelling study. Unfortunately, only two stations fall in the tidal section of the Scheldt, considered in this study.

A second set of data was used: measurements of culturable faecal coliforms made by the VMM at one station in the Scheldt River (Zele) and three locations in the estuary very close to each other (around Doel). The faecal coliform concentrations were converted into culturable *E. coli* concentrations by multiplying the faecal coliform data by 0.77; this value is the average ratio between *E. coli* and faecal coliform numbers measured in river water samples (Garcia-Armisen et al., 2007). The VMM measurements span different periods, ranging from 2000 to 2008, and hence do not exactly correspond to the modelled period. For these reasons, the VMM measurements should be regarded with some caution.

4. Results and discussion

4.1. Reference simulation

4.1.1. Total E. coli concentration

The results of the reference simulation are shown in Fig. 3, as a profile along the axis of the Scheldt River and Estuary. In the 1D model part (river), the values represent section-averaged *E. coli* concentrations; in the 2D model part (estuary), the concentrations are shown along a path in the estuary following the main channel (thalweg). The simulated *E. coli* concentrations from 25 March 2007 to 15 June 2008 (i.e. the period covered by the monthly measurements) are summarised by the median value at each location, as well as the interquartile range and the minimal and maximal values.

Both the simulated median *E. coli* concentration and the range of temporal variability correspond relatively well to the observations. In the estuarine part (downstream ~ km100), there is more difference between the model and the field data: the model predicts a steeper decrease than the data suggest. However, it should be noted that, in this part, the data are less representative (because they represent single samples during one cruise or because they are actually faecal coliform data and some of them were measured before the simulation period).

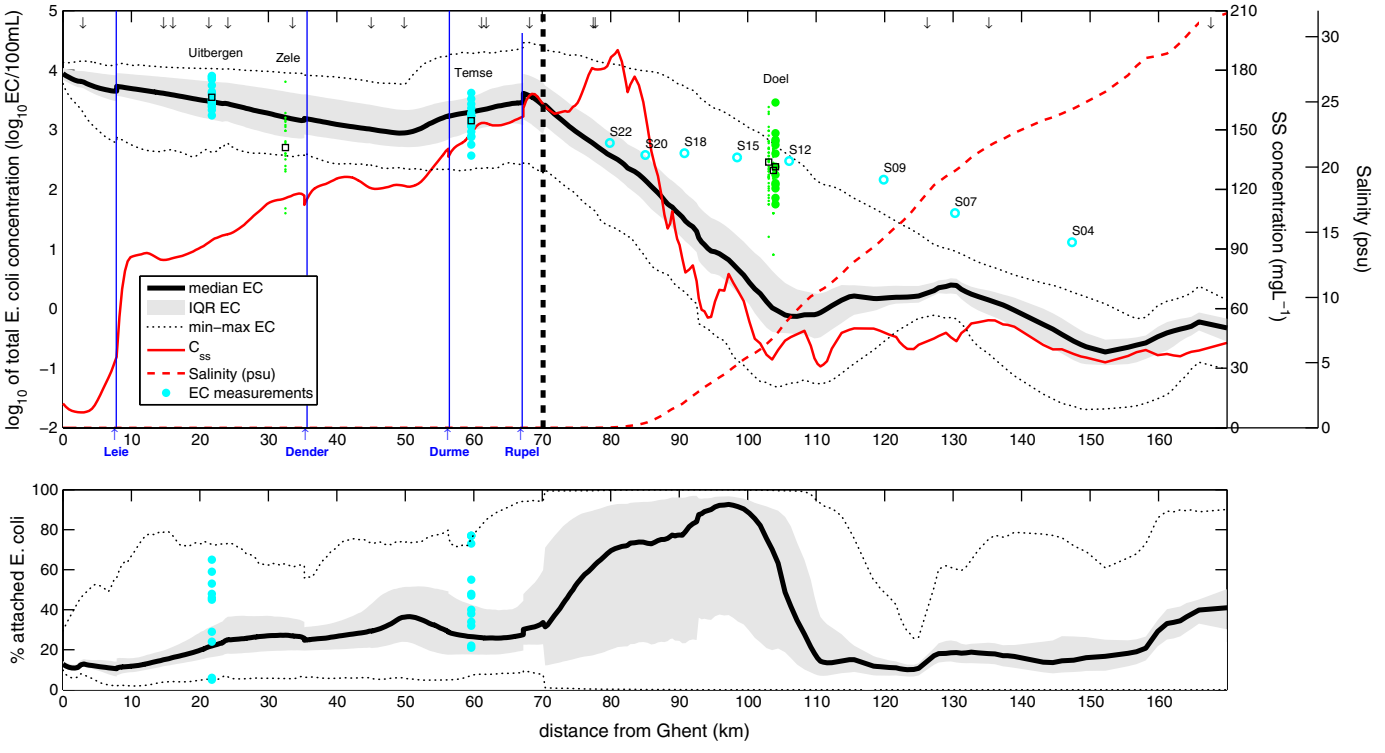

Fig. 3. Reference simulation results. Upper panel: $\log_{10}$ of total *E. coli* concentrations [$\log_{10}$*E. coli* (100 mL)$^{-1}$] and SS concentration [mg L^{-1}]; lower panel: proportion of *E. coli* attached to SS [%]. Model results are summarised by their median value (thick black line), interquartile range (grey area) and minimum–maximum (black dotted lines, not always within scale) over the simulated period. Median simulated SS concentration is shown as the red line, salinity as dotted red line. Measurements are depicted as dots: the full cyan dots stand for data from the monthly monitoring (Ouattara et al., 2011), the squares indicate the median value for our two monitoring stations, the green dots show VMM data, the smaller dots are measurements taken at a time not covered by the simulation period, and the open cyan circles indicate measurements made during an estuarine cruise on 12 February 2008. Spatial reference points are added in the upper panel: the confluence points of the tributaries (blue vertical lines) and approximate location of WWTP outlets (arrows at the top). The thick black vertical dashed line indicates the connection between the 1D (left) and the 2D model (right). (For interpretation of the references to colour in this figure legend, the reader is referred to the web version of this article.)

An important observation is that the station Temse is clearly influenced by the highly contaminated waters coming from the Rupel River, which carries the wastewaters from the city of Brussels. The only way to reproduce these elevated *E. coli* concentrations in the Scheldt upstream of the Rupel is by taking into account the tides, because this process periodically pushes water upstream. Another striking observation is that the WWTPs located along the modelled domain do not seem to contribute significantly to the contamination in the study domain, i.e. most of the *E. coli* enters from upstream or from tributaries.

A correct description of the *E. coli* dynamics in the tidal Scheldt is complicated because of the multiple complex processes acting simultaneously. The above results clearly show that the major challenge is to accurately represent the main peak of concentration originating from the Rupel–Zenne Rivers, and the subsequent concentration decrease in the Scheldt Estuary. To complicate things even more, this zone coincides with the maximum turbidity zone or MTZ (see profile of C_{SS} in Fig. 3), and therefore the sediment particles are likely to be subject to a complex succession of settling and resuspension cycles. In an attempt to gain more insight in the relative importance of the different processes acting on the *E. coli* concentrations along the Scheldt, the fluxes of settling, resuspension and mortality were quantified (results not shown). A general feature is that the mortality rates are quite small but relatively constant throughout the domain. The sediment-related fluxes of settling and resuspension are larger and more variable. Especially in the MTZ the relative importance of resuspension and settling is extremely erratic. This makes it rather difficult to make any statements about the relative importance of the different processes and their role in the simulated *E. coli* concentrations. The model sensitivity to the sediment-related processes will be further investigated in Section 4.2.

The fact that virtually no *E. coli* bacteria reach the estuary mouth seems to be a robust result (e.g. independent of hydrological conditions) as even the maximal simulated values are extremely low. Downstream of km 100 the median concentration fluctuates around 1 EC/100 mL; the maximal concentration drops below 10 EC/100 mL at km 130. Therefore, we can state that the Scheldt is not a significant source of faecal pollution for the adjacent Dutch–Belgian coastal zone. The Scheldt Estuary effectively acts as a cleaning filter with respect to faecal pollution. This is caused by the combined effect of dilution and decay of the *E. coli* bacteria in each of their forms (free, attached to SS, in the bottom sediments), and the relatively long residence time in the Scheldt Estuary (de Brauwere et al., 2011a; de Brye et al., 2012).

The range of temporal variability associated with these kinds of contaminants is well-known to be quite large and difficult to reproduce in a model as they are linked to generally unknown fluctuations in the source inputs. The reason why here we are able to reproduce a reasonable range of variability is that in this domain the tide is the principal cause of temporal variability (de Brauwere et al., 2011b) and the tides are explicitly represented in the model. Considering that (i) none of the parameters has been tuned and (ii) the upstream concentrations (another forcing which has been shown to have a major influence on the (median) concentrations inside the tidal domain, cf. de Brauwere et al. (2011a, 2011b)) are directly coming from the SENEQUE-EC model simulations, these overall results are satisfactory.

4.1.2. Fraction of attached E. coli

By splitting the *E. coli* in free and attached species we are able to study not only the total concentration but also the partitioning between the two types. Although the free and attached *E. coli* in the model do not interact, they are present in different amounts in the sources and subject to different vertical processes and decay, and therefore their relative abundance in the water column will vary in time and space. In Fig. 3 also the proportion of attached *E. coli* is shown along the Scheldt axis. The median fraction of attached bacteria ranges from roughly 10 to 90%, but again the temporal variability at a given point is huge: between km 70 and 110 the simulated attachment fraction covers virtually all values from 0 to 100%. In this zone, the median % of attached *E. coli* is higher than elsewhere. This corresponds to the decrease of total concentration and is related to the fact that no important sources or tributaries introduce bacteria in this part of the domain. In other words, the bacteria present between km 70 and 110 principally come from further upstream. As the free *E. coli* are set to decay at a faster rate than those attached to particles, the latter type will be more and more abundant. This is probably amplified by the frequent stays of the attached *E. coli* on the bottom (cf. Delhez and Wolk, 2013, for an estimation of the residence time of sediment-adsorbed constituents on the bottom of the Scheldt Estuary) where the *E. coli* survive even longer. The simulated decrease in the attachment fraction continuing downstream is probably due to the few WWTPs present along the estuary, injecting "fresh" *E. coli*, both free and attached. This being said, the total concentrations at these locations are almost zero, so interpretation of what happens is of no real significance.

The huge variability in terms of attachment ratio in the downstream part is probably a consequence of the tidally driven deposition and erosion cycles. As most of the *E. coli* are attached to particles, when they settle to the bottom only the few free *E. coli* are left in the water column (low attachment ratio). The next tidal cycle, the *E. coli* on the bottom are resuspended such that again the attached *E. coli* are the overwhelming type (almost 100% attachment ratio). This being said, we cannot validate the results in terms of attachment fraction because field measurements of the free/attached *E. coli* proportion are lacking for the estuarine zone.

4.2. Model sensitivity

In this section we further discuss the aspects of the model that could be improved and investigate the sensitivity of the model with respect to possible changes.

(i) The current model set-up assumes that free and attached *E. coli* do not interact. The arguments for making this hypothesis were given in Section 2.4. It is hardly possible to assess the impact of this hypothesis because there is no consistent information on actual adsorption–desorption and biological attachment kinetics. The existing studies on this subject are usually restricted to the core scale and none of them have been judged satisfactory to use on a larger scale (Pachepsky et al., 2006). In other words, these processes are represented in a simplified way in the current model, but this is true for all current faecal contamination models.

(ii) Although a full assessment of the sensitivity of the *E. coli* simulations with respect to the choices in the SS module is outside the scope of the current study, we would like to discuss a few points. The SS module (Gourgue et al., 2013) has been specifically designed to be used as "carrier" for environmental contaminants (*E. coli*, metals, etc.). Therefore, the aims were to keep the model formulations as simple as possible (keep the computation cost low) while accurately representing the main dynamical and spatial features of SS in the Scheldt tidal continuum. One important simplification is that the module only considers one "bulk" class of (cohesive) sediment particles. Considering several particle size classes could further improve the quality of the SS model, especially inside the estuary and in the adjacent coastal zone where fluvial and marine sediments mix. However, it is doubtful that these improvements would significantly impact the *E. coli* simulations since their concentration is very low in this zone under marine influence. Furthermore, it would require knowing the particle class dependent attachment of the bacteria. A second feature of the SS module that probably influences the *E. coli* results is the fact that the simulated MTZ is shifted slightly towards upstream. This may explain why the *E. coli* decrease in this zone is a little too steep. With higher SS concentrations, the attached *E. coli* concentrations could indeed be increased in this zone.

(iii) In order to further assess the impact of the deposition and erosion processes a sensitivity run was performed without them ("noDE"). The results are compared to the reference simulation in Fig. 4b. Surprisingly, in the new simulation the concentrations are generally increased. Although the concentration peak is therefore higher, the concentration in the MTZ reaches quasi-zero values approximately at the same location. Furthermore, when comparing the simulated timeseries at given points (results not shown), it is clear that the settling–resuspension processes do not have the effect to increase the local total *E. coli* concentration variability (either it is not affected or it is reduced). In other words, the observed variability in the tidal Scheldt is not driven by the deposition–erosion processes. Instead, the tides are probably the main cause of local variability, as already suggested by de Brauwere et al. (2011b). Although the "noDE" simulation produces results not so different from the reference simulations, the first seems less compatible with the observations at Temse. Therefore, we conclude that the explicit representation of the settling–resuspension processes improves the simulations, although the differences are not very large. In addition, the explicit representation of the settling–resuspension processes (and the free and attached bacteria) also increases the insight in the system and offers more interpretation potential — even if the field data reproduction is not improved much.

(iv) The 10-day time step of the upstream SENEQUE-EC model (i.e. of the upstream boundary conditions) could cause an underestimation of the simulated variability inside the SLIM-EC2 model. However, the long-term median behaviour and range of variability are hardly influenced. This has been tested by adding artificial "variability" (normally distributed random noise with a standard deviation of 50%) to the boundary conditions provided by SENEQUE-EC, while keeping the mean value identical (see Fig. 4a for an example). The results are compared to the reference simulation in Fig. 4b–c and clearly show that the effect is negligible (both on median and variability), except for the range of variability in the vicinity of the boundaries. Remarkably, even the timeseries at given points are hardly influenced (results not shown). These results may seem surprising but they are in line with the previously made observation that the tides are the major driver of the *E. coli* concentration variability in the tidal Scheldt. They effectively mix the water, consequently smoothing out the high frequency variability of the upstream concentrations. Note that this result only points out the insensitivity with respect to the *variability* of the upstream boundary conditions — the *mean* values of the boundary concentrations are still of great importance.

(v) The constant *E. coli* concentration and attachment ratio in a WWTP source are clearly assumptions which do not correspond to reality. In reality, the flow rate and the *E. coli* concentration, as well as the fraction of attached bacteria in the discharge vary in time and space, according to e.g. weather conditions, origin of the wastewater and applied treatments. Spatial variation (i.e. individual WWTP information) was taken into account as much as possible, based on WWTP-specific data of water discharge and typical *E. coli* concentrations per type of treatments applied (cf. Section 2.5). Yet, no temporal variation is included because no temporally resolved discharge data (let alone *E. coli* concentration data) exist for all the WWTPs in this domain (more than 480 for the whole Scheldt catchment). This being said, de Brauwere et al. (2011b) and the current study show that the WWTP point sources only have a secondary effect on the simulated concentrations in the tidal part of the watershed, justifying this simplified representation in the model, especially when looking at long-term effects.

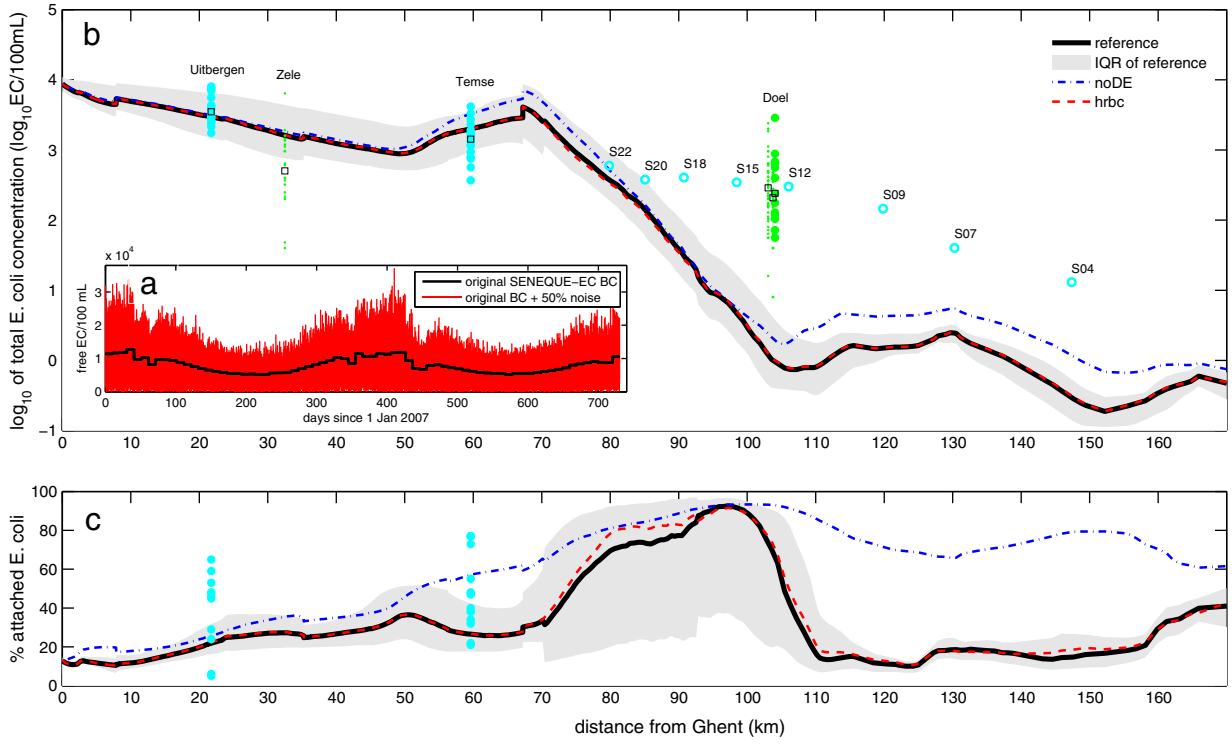

Fig. 4. Sensitivity on boundary conditions and inclusion of vertical processes. (a) Example of highly variable synthetic boundary condition (here: for free *E. coli* at the Scheldt boundary). In black the original boundary conditions, in red the "high-resolution boundary condition" (hrBC) after adding random normally distributed noise with 50% standard deviation. (b) Comparison between median total concentration by the reference simulation (black) and sensitivity runs: highly variable upstream boundary conditions (hrBC, in dotted red) and no deposition–erosion (noDE, in dash-dotted blue). Results represent medians over the same 15 months simulation period as in Fig. 3. Data are represented by dots, see caption of Fig. 3. For the sake of clarity, the 1D–2D connection, tributaries and WWTPs are not indicated, but can be seen in Fig. 3. (c) Comparison for the attachment fraction. (For interpretation of the references to colour in this figure legend, the reader is referred to the web version of this article.)

(vi) The decay constants used in the current study rely on a number of assumptions (Section 2.4) and hence are associated with uncertainty. In order to assess the sensitivity of the model results to changing decay constants, we performed five additional sensitivity runs: we respectively increased and decreased the k_f^{20} and k_a^{20} by a factor of 10, and performed a run with $k_b^{20} = 1.25 \times 10^{-6}\ s^{-1}$ (i.e. as in the upstream model SENEQUE-EC, cf. Ouattara et al. (2013)). The results of these simulations are shown in Fig. 5. The upper panel shows the resulting median total *E. coli* concentration profiles. As expected, reducing the k^{20} values has the effect to increase the simulated *E. coli* concentrations, and vice versa. For k_a and k_b the changes in total concentrations with respect to the reference simulation are not spectacular (notwithstanding the large range of parameter variation), while the simulation results seem much more sensitive to changes in k_f. These tests also show that only a decrease of k_f will result in higher estuarine concentrations (i.e. for km >90). Now looking at the sensitivity of the attachment ratio (lower panel of Fig. 5), it becomes clear that a better representation in terms of total concentrations does not imply a more realistic simulation of the % attached bacteria. For instance, decreasing k_f (which would improve the estuarine concentration decline) would decrease the attachment fraction too much compared to the scarce observations. Another simulation we want to briefly discuss is the one with non-zero k_b^{20} (the actual value used by SENEQUE-EC in the upstream catchment). This simulation both gives a worse reproduction of the observed concentrations (underestimation at Uitbergen and of the estuarine decrease), and attachment ratios (clear underestimation at Temse). These results are an additional justification for setting $k_b^{20} = 0$.

In summary, we believe that – given the available observations – the current set-up covers the most important processes governing the long-term *E. coli* concentration distribution in the Scheldt. Therefore, the model can be a useful tool to perform scenario studies within this long-term time frame.

4.3. Wastewater management scenarios

Two different scenarios regarding the wastewater management in the Brussels area were tested in this study. The Brussels region wastewater is treated by two WWTPs: Brussels North WWTP (1.1×10^6 inhabitant-equivalents) and Brussels South WWTP (3.6×10^5 inhabitant-equivalents). The treatment line in Brussels South WWTP includes a primary settling followed by an activated sludge process. The large Brussels North WWTP has two treatment lines: a biological treatment line (including activated sludge with removal of N and P) and a treatment line in which only a primary settling is applied. The latter one is devoted to treat the excess of volume which cannot be treated by the biological line when the discharge reaching the WWTP is too high (typically during rain events). On average, the volume treated in the biological line represents roughly 90% of the total volume reaching the WWTP. In addition, during rain events in the Brussels area, due to an insufficient capacity of the sewer system, untreated wastewater is released directly in the Zenne River by combined sewer overflows.

Brussels lies upstream of the SLIM domain and its principal wastewater pathways are explicitly represented in the SENEQUE-EC model (Ouattara et al., 2013). The management scenarios are thus explicitly implemented in SENEQUE-EC and their effect is traced through the tidal domain by adapting the Zenne boundary conditions of SLIM-EC2 (cf. Fig. 1).

A "best case" scenario was imagined considering that all of the Brussels wastewater is treated by the two WWTPs (no more combined sewer overflows) and disinfected by UV irradiation, which should reduce the *E. coli* input by several orders of magnitude (Servais et al., 2007b).

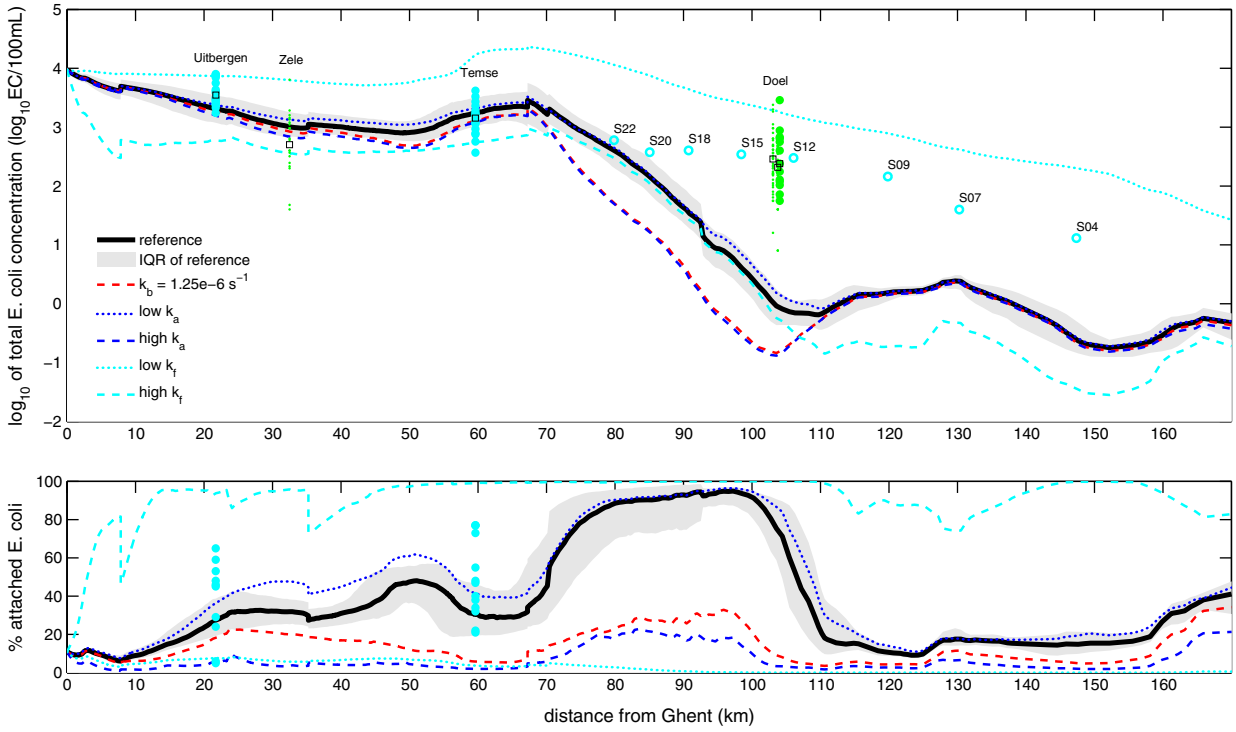

Fig. 5. Mortality rate sensitivity. Comparison between reference simulation (black) and simulation with altered mortality rate. One mortality rate (i.e. of the free, attached or bottom bacteria) is changed at a time. "High" means 10 times higher than in the reference simulation, while "low" implies the reference value divided by 10. The longitudinal profiles represent medians of 2-month simulations (26 March–26 May 2007). All available measurements are indicated as dots (see Fig. 3 and text for more details). For the sake of clarity, the 1D–2D connection, tributaries and WWTPs are not indicated, but can be seen in Fig. 3.

The "worst case" scenario assumes that none of the Brussels wastewater is treated. Note that this was actually the real situation before 2000, as then the first Brussels WWTP (Brussels South) was built. It was not until 2007, when the Brussels North WWTP opened, that all wastewater was treated, at least during dry weather situations. The worst case scenario thus gives an idea not only of the situation before 2000, but also of the impact of possible breakdowns of the WWTPs (as happened e.g. in the Brussels North WWTP during 10 days in December 2009).

Fig. 6 shows the changed Zenne boundary concentrations. Surprisingly, the worst case scenario produces *E. coli* concentrations which are less than one order of magnitude superior to the reference situation concentrations. This illustrates that in the reference situation a significant proportion of the wastewater is not or hardly treated. Furthermore, the part that is treated does not undergo a specific treatment to remove microbiological pollutants (disinfection stage), resulting in an *E. coli* concentration decrease of only ~2 orders of magnitude.

4.3.1. Best case scenario

In the best case scenario, the improved water quality of the Zenne (Fig. 6) has a clear beneficial impact on the *E. coli* concentrations in the Scheldt as well (Fig. 7). Between km 0 and 50, there is no difference with the reference situation. But from km 50 on, the contamination in the best case scenario is significantly reduced. This confirms the above statement that the zone downstream of km 50 is heavily influenced by the contaminated Zenne water. In summary, these results show that investing in a better Brussels wastewater management has a significant beneficial effect on the downstream water quality, as far as the Scheldt, some 35 km away.

In the best case scenario the fraction of attached bacteria is substantially reduced in parts of the domain (Fig. 7b). At first it may seem to be related to the fact that the water entering from the Zenne contains much less attached *E. coli* in this scenario than in the reference situation (cf. Fig. 6b); a phenomenon which is due to the fact that the diffuse sources are dominant and these are characterised by a much lower fraction of attached *E. coli* (cf. Fig. 3 in Ouattara et al. (2013)). However, Fig. 7a and b show that the Zenne (or Rupel) water does not significantly influence either total concentrations or attachment ratios in the Scheldt in this scenario. Therefore, our hypothesis is that the local WWTP inputs have a more significant influence as the total in situ concentration is lower.

4.3.2. Worst case scenario

In line with the expectations there is a significant concentration increase between the worst case and reference simulations and it is mainly visible between km 40 and 90. Median concentrations rise to 16,000 *E. coli* $(100\ mL)^{-1}$, but maximal values reach as much as 100,000 *E. coli* $(100\ mL)^{-1}$ (not shown). Considering this substantial concentration increase, it is surprising that the extent of the influenced zone is actually barely larger than in the reference situation. In other words, it seems that beyond km 100 any contamination coming from the Zenne is removed, independently of its actual concentration. Regarding the attachment ratios along the Scheldt, there are small differences with the reference simulation, but overall they are very similar.

5. Summary and conclusions

This study illustrates the potential of an integrated multi-scale model having varying spatial and temporal resolutions depending on

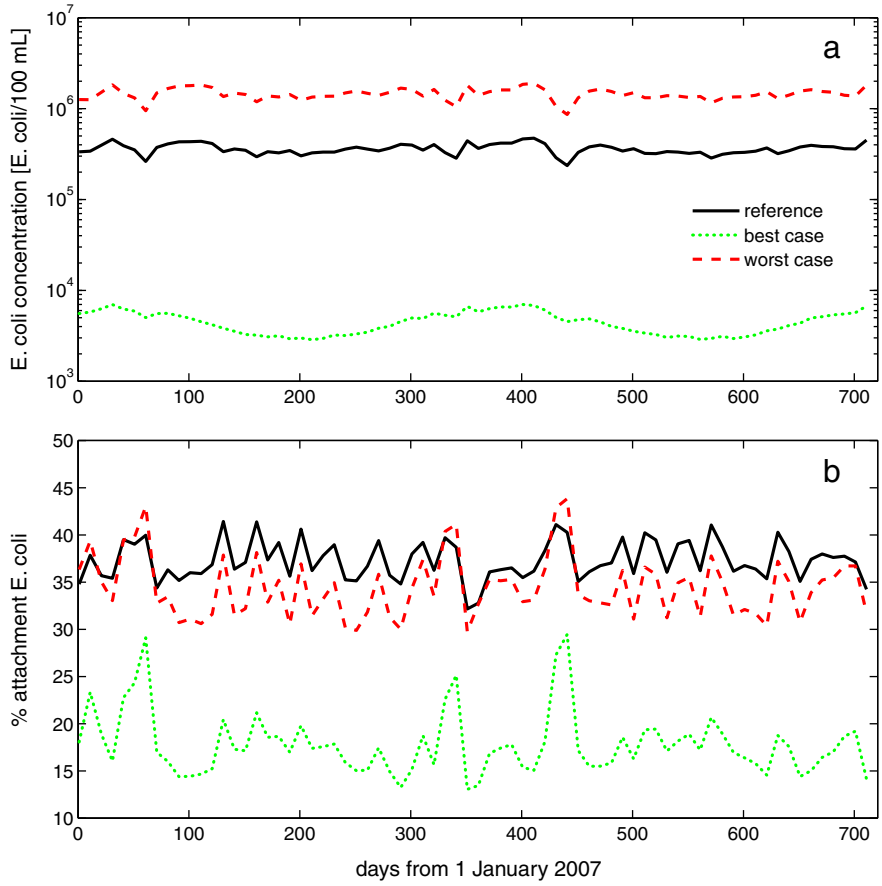

Fig. 6. *E. coli* concentrations (a) and attachment ratios (b) at the Zenne boundary of the SLIM domain, as produced by SENEQUE-EC (Ouattara et al., 2013), for the reference simulation (full black line), best case scenario (green dotted line) and worst case scenario (red dashed line). (For interpretation of the references to colour in this figure legend, the reader is referred to the web version of this article.)

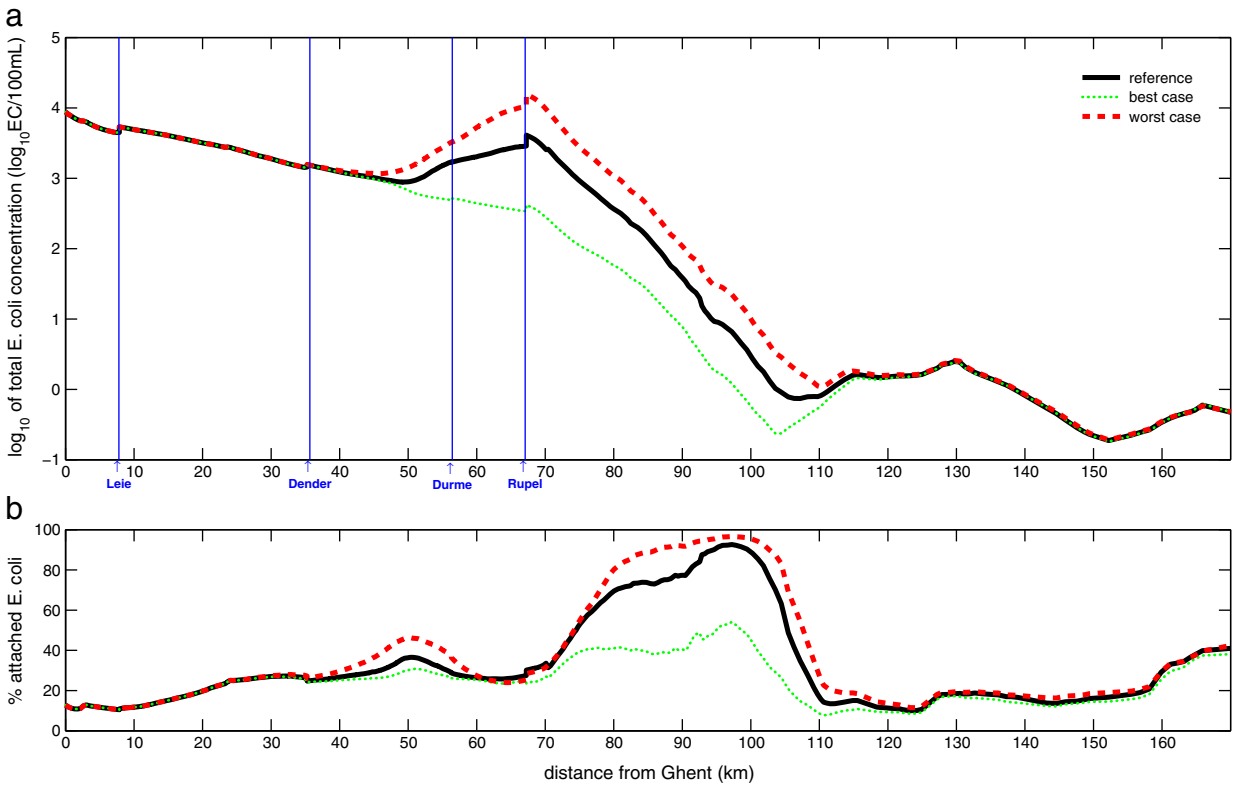

Fig. 7. Comparison of the reference simulation (black) with the best case (green dotted) and worst case (red dashed) scenarios, in terms of (a) median total *E. coli* concentrations and (b) median fraction of attached *E. coli*. Tributaries are indicated by vertical blue lines. WWTP outfalls and 1D–2D model connection are not indicated but can be found in Fig. 3. (For interpretation of the references to colour in this figure legend, the reader is referred to the web version of this article.)

the prominent processes and morphology of the domain. Indeed, for the upstream watershed where many smaller rivers and streams are present and the tides absent, a watershed model is used with coarse time resolution (SENEQUE-EC); while for the tidal rivers a tidal model (SLIM-EC2) of 1D river sections is used, and finally when the Scheldt River widens to become an estuary and finally reaches the North Sea the 2D version of the tidal model is used.

In addition to the novel integrated modelling, another methodological improvement of SLIM-EC2 regards the partitioning of the *E. coli* pool into free-floating and attached to particles. The dynamics of the latter are directly linked to the SS dynamics which were also modelled explicitly. Sediment attachment has been accepted in recent years to be an important factor of the observed *E. coli* dynamics (Pachepsky and Shelton, 2011), and especially in the highly turbid Scheldt this seems to be a realistic hypothesis. Moreover, the main MTZ of the estuary corresponds to the zone where the Scheldt is severely contaminated by Rupel water and where this contamination is removed by natural decay. It was the combination of these facts that motivated us for this model refinement.

With these new model improvements the observed *E. coli* concentration patterns and temporal variability in the tidal Scheldt are well reproduced. Although the improvement is only minor compared to the previous model SLIM-EC, it has to be kept in mind that the new model has not been tuned. While for SLIM-EC, there was some tuning freedom for the decay rate and boundary conditions, these are now fixed due to the coupling with SENEQUE-EC. The only parameter that we allowed to modify compared to SENEQUE-EC was the bottom mortality rate (as discussed above). Furthermore, the explicit representation of the settling–resuspension processes, as well as the partitioning of the total bacteria pool in free and attached bacteria, increases the possible insight in the system and allows for more mechanistic interpretations (SLIM-EC only considered one bacteria pool and no explicit resuspension). In addition, the available measurements to validate the model are rather limited and associated with some uncertainty. Yet, several sensitivity tests enabled to gain more confidence in the robustness of the results.

This new model set-up allows to perform long-term (a few months–years) impact studies integrating the whole Scheldt basin and adjacent North Sea. For instance, different faecal contamination scenarios can be considered and their impact can be traced all along the Scheldt continuum. In this study, illustrative "best case" and "worst case" scenarios for the Brussels wastewater management were studied. These scenarios clearly showed that the current situation is not much better than the worst case scenario, confirming the negative impact of the non-negligible amounts of partially treated and untreated wastewater released in the Zenne. Remarkably, even in the worst case scenario the huge *E. coli* concentrations are removed rapidly from the water column by natural decay, such that the contaminated zone is hardly larger than in the reference situation. In other words, even in a worst case situation concerning Brussels' wastewater, the Scheldt Estuary is an efficient filter and no significant amounts of *E. coli* are released in the North Sea by this route. On the other hand, in the best case scenario the concentrations are reduced enough so that the Zenne does not significantly contaminate the Scheldt anymore.

Acknowledgements

The present work was carried out in the framework of the TIMOTHY project (Interuniversity Attraction Pole, IAP 6/13), funded by the Belgian Science Policy (BELSPO). Anouk de Brauwere is a post-doctoral researcher with the Fonds National de la Recherche Scientifique (F.R.S.-FNRS). N.K. Ouattara had a doctoral grant from the Ivory Coast Government and benefited from a doctoral fund from "Fonds Van Buuren". Computational resources have been provided by the high-performance computing facilities of the Université catholique de Louvain (CISM/UCL) and the Consortium des Equipements de Calcul Intensif en Fédération

Wallonie Bruxelles (CECI) funded by the Fond de la Recherche Scientifique de Belgique (F.R.S.-FNRS). The development of SLIM is performed under the auspices of the contract ARC 10/15-028, which is funded by the Communauté Française de Belgique.

Appendix A. One-dimensional equations for the *E. coli* dynamics

The one-dimensional equations used to describe the *E. coli* fate in the rivers are

$$\frac{\partial}{\partial t}\left(AC_f\right)+\frac{\partial}{\partial x}\left(AuC_f\right)=\frac{\partial}{\partial x}\left(A\kappa\frac{\partial}{\partial x}C_f\right)+AR_f, \tag{A1}$$

$$\frac{\partial}{\partial t}\left(AC_aC_{SS}\right)+\frac{\partial}{\partial x}\left(AuC_aC_{SS}\right)=\frac{\partial}{\partial x}\left(A\kappa\frac{\partial}{\partial x}\left(C_aC_{SS}\right)\right)+AR_a, \tag{A2}$$

$$\frac{\partial}{\partial t}\left(bC_{sb}C_b\right)=bR_b, \tag{A3}$$

where x is the along-river coordinate [m], A is the cross-sectional area [m^2] and b is the river width [m]. The source-sink terms R_f, R_a, and R_b are the same as in the two-dimensional equations (Eqs. (12), (14), (15)) given that H is set $= A/b$.

References

Baeyens W, van Eck B, Lambert C, Wollast R, Goeyens L. General description of the Scheldt Estuary. Hydrobiologia 1998;366:1–14.

Bai S, Lung W-S. Modeling sediment impact on the transport of fecal bacteria. Water Res 2005;39:5232–40.

Barcina I, Arana I, Iriberri J, Egea L. Factors affecting the survival of *E. coli* in a river. Hydrobiologia 1986;141:249–53.

Beaudeau P, Tousset N, Bruchon F, Lefevre A, Taylor HD. In situ measurement and statistical modelling of *Escherichia coli* decay in small rivers. Water Res 2001;35:3168–78.

Bedri Z, Bruen M, Dowley A, Masterson B. A three-dimensional hydro-environmental model of Dublin Bay. Environ Model Assess 2011;16:369–84. http://dx.doi.org/10.1007/s10666-011-9253-7.

Bougeard M, Le Saux J-C, Pérenne N, Baffaut C, Robin M, Pommepuy M. Modeling of *Escherichia coli* fluxes on a catchment and the impact on coastal water and shellfish quality 1. J Am Water Res Assoc 2011;47:350–66. http://dx.doi.org/10.1111/j.1752-1688.2010.00520.x.

Bucci V, Vulić M, Ruan X, Hellweger FL. Population dynamics of *Escherichia coli* in surface water. J Am Water Res Assoc 2011;47:611–9. http://dx.doi.org/10.1111/j.1752-1688.2011.00528.x.

Bucci V, Hoover S, Hellweger F. Modeling adaptive mutation of enteric bacteria in surface water using agent-based methods. Water Air Soil Pollut 2012;223:2035–49. http://dx.doi.org/10.1007/s11270-011-1003-6.

Cho KH, Cha SM, Kang JH, Lee SW, Park Y, Kim JW, et al. Meteorological effects on the levels of fecal indicator bacteria in an urban stream: a modeling approach. Water Res 2010;44:2189–202. http://dx.doi.org/10.1016/j.watres.2009.12.051.

Connolly JP, Blumberg AF, Quadrini JD. Modeling fate of pathogenic organisms in coastal waters of Oahu, Hawaii. J Environ Eng 1999;125:398–406. http://dx.doi.org/10.1061/(asce)0733-9372(1999)125:5(398).

Craig DL, Fallowfield HJ, Cromar NJ. Use of microcosms to determine persistence of *Escherichia coli* in recreational coastal water and sediment and validation with in situ measurements. J Appl Microbiol 2004;96:922–30. http://dx.doi.org/10.1111/j.1365-2672.2004.02243.x.

de Brauwere A, de Brye B, Blaise S, Deleersnijder E. Residence time, exposure time and connectivity in the Scheldt Estuary. J Mar Syst 2011a;84:85–95. http://dx.doi.org/10.1016/j.jmarsys.2010.10.001.

de Brauwere A, de Brye B, Servais P, Passerat J, Deleersnijder E. Modelling *Escherichia coli* concentrations in the tidal Scheldt River and Estuary. Water Res 2011b;45:2724–38. http://dx.doi.org/10.1016/j.watres.2011.02.003.

de Brauwere A, Ouattara NK, Servais P. Modeling fecal indicator bacteria concentrations in natural surface waters: a review. Crit Rev Environ Sci Technol 2013. [in press].

de Brye B. Development of a multiscale finite-element model for river–sea continua: application to the Scheldt (Belgium/The Netherlands) and the Mahakam (Indonesia). Institute of Mechanics, Materials and Civil Engineering (iMMC). Louvain-la-Neuve: Université catholique de Louvain; 2011.

de Brye B, de Brauwere A, Gourgue O, Kärnä T, Lambrechts J, Comblen R, et al. A finite-element, multi-scale model of the Scheldt tributaries, River, Estuary and ROFI. Coast Eng 2010;57:850–63. http://dx.doi.org/10.1016/j.coastaleng.2010.04.001.

de Brye B, Schellen S, Sassi M, Vermeulen B, Kärnä T, Deleersnijder E, et al. Preliminary results of a finite-element, multi-scale model of the Mahakam Delta (Indonesia). Ocean Dyn 2011;61:1107–20. http://dx.doi.org/10.1007/s10236-011-0410-y.

de Brye B, de Brauwere A, Gourgue O, Delhez EJM, Deleersnijder E. Water renewal timescales in the Scheldt Estuary. J Mar Syst 2012;94:74–86. http://dx.doi.org/10.1016/j.jmarsys.2011.10.013.

Delhez ÉJM, Wolk F. Diagnosis of the transport of adsorbed material in the Scheldt Estuary: a proof of concept. J Mar Syst 2013. http://dx.doi.org/10.1016/j.jmarsys.2012.01.007. [in press].

Dorner SM, Anderson WB, Slawson RM, Kouwen N, Huck PM. Hydrologic modeling of pathogen fate and transport. Environ Sci Technol 2006;40:4746–53. http://dx.doi.org/10.1021/es060426z.

Einstein HA, Krone RB. Experiments to determine modes of cohesive sediment transport in salt water. J Geophys Res 1962;67. http://dx.doi.org/10.1029/JZ067i004p01451.

Fletcher M. Bacteria attachment in aquatic environments: a diversity of surfaces and adhesion strategies. Bacterial adhesion: molecular and ecological diversity. John Wiley Publication; 1996.

Flint KP. The long-term survival of *Escherichia coli* in river water. J Appl Bacteriol 1987;63:261–70.

Gao G, Falconer RA, Lin B. Numerical modelling of sediment–bacteria interaction processes in surface waters. Water Res 2011;45:1951–60. http://dx.doi.org/10.1016/j.watres.2010.12.030.

Garcia-Armisen T, Servais P. Partitioning and fate of particle-associated *E. coli* in river waters. Water Environ Res 2009;81:21–8. http://dx.doi.org/10.2175/106143008x304613.

Garcia-Armisen T, Thouvenin B, Servais P. Modelling faecal coliforms dynamics in the Seine estuary, France. Water Sci Technol 2006;54:177–84. http://dx.doi.org/10.2166/wst.2006.466.

Garcia-Armisen T, Prats J, Servais P. Comparison of culturable fecal coliforms and *Escherichia coli* enumeration in freshwaters. Can J Microbiol 2007;53:798–801.

Gourgue O, Deleersnijder E, White L. Toward a generic method for studying water renewal, with application to the epilimnion of Lake Tanganyika. Estuar Coast Shelf Sci 2007;74:628–40. http://dx.doi.org/10.1016/j.ecss.2007.05.009.

Gourgue O, Baeyens W, Chen MS, de Brauwere A, de Brye B, Deleersnijder E, et al. A depth-averaged two-dimensional sediment transport model for environmental studies in the Scheldt Estuary and tidal river network. J Mar Syst 2013. http://dx.doi.org/10.1016/j.jmarsys.2012.05.004. [in press].

Heberger MG, Durant JL, Oriel KA, Kirshen PH, Minardi L. Combining real-time bacteria models and uncertainty analysis for establishing health advisories for recreational waters. J Water Res Plan Manag —Asce 2008;134:73–82. http://dx.doi.org/10.1061/(asce)0733-9496(2008)134:1(73).

Hellweger FL, Masopust P. Investigating the fate and transport of *Escherichia coli* in the Charles River, Boston, using high-resolution observation and modeling. J Am Water Resour Assoc 2008;44:509–22. http://dx.doi.org/10.1111/j.1752-1688.2008.00179.x.

Hipsey MR, Antenucci JP, Brookes JD. A generic, process-based model of microbial pollution in aquatic systems. Water Resour Res 2008;44. [doi:W0740810.1029/2007wr006395].

Jamieson R, Joy DM, Lee H, Kostaschuk R, Gordon R. Transport and deposition of sediment-associated *Escherichia coli* in natural streams. Water Res 2005a;39:2665–75. http://dx.doi.org/10.1016/j.watres.2005.04.040.

Jamieson RC, Joy DM, Lee H, Kostaschuk R, Gordon RJ. Resuspension of sediment-associated *Escherichia coli* in a natural stream. J Environ Qual 2005b;34:581–9.

Kärnä T, Legat V, Deleersnijder E. A baroclinic discontinuous Galerkin finite element model for coastal flows. Ocean Model 2013;61:1–20.

Lambrechts J, Hanert E, Deleersnijder E, Bernard PE, Legat V, Remacle JF, et al. A multi-scale model of the hydrodynamics of the whole Great Barrier Reef. Estuar Coast Shelf Sci 2008;79:143–51. http://dx.doi.org/10.1016/j.ecss.2008.03.016.

Le Hir P, Guillaud JF, Bassoullet P, L'Yavanc J. Application d'un modèle sédimentaire au devenir des contaminants particulaires. La Mer et les Rejets Urbains. Bendor: IFREMER, Actes de Colloques; 1990. p. 205–20.

Liu W-C, Huang W-C. Modeling the transport and distribution of fecal coliform in a tidal estuary. Sci Total Environ 2012;431:1–8. http://dx.doi.org/10.1016/j.scitotenv.2012.05.016.

Liu L, Phanikumar MS, Molloy SL, Whitman RL, Shively DA, Nevers MB, et al. Modeling the transport and inactivation of *E. coli* and enterococci in the near-shore region of Lake Michigan. Environ Sci Technol 2006;40:5022–8. http://dx.doi.org/10.1021/es060438k.

Manache G, Melching CS, Lanyon R. Calibration of a continuous simulation fecal coliform model based on historical data analysis. J Environ Eng 2007;133:681–91. http://dx.doi.org/10.1061/(asce)0733-9372(2007)133:7(681).

Manning AJ, Langston WJ, Jonas PJC. A review of sediment dynamics in the Severn Estuary: influence of flocculation. Mar Pollut Bull 2010;61:37–51. http://dx.doi.org/10.1016/j.marpolbul.2009.12.012.

McCorquodale JA, Georgiou I, Carnelos S, Englande AJ. Modeling coliforms in storm water plumes. J Environ Eng Sci 2004;3:419–31. http://dx.doi.org/10.1139/s03-055.

Menon P, Billen G, Servais P. Mortality rates of autochthonous and fecal bacteria in natural aquatic ecosystems. Water Res 2003;37:4151–8. http://dx.doi.org/10.1016/s0043-1354(03)00349-x.

Okubo A. Oceanic diffusion diagrams. Deep-Sea Res 1971;18:789–802.

Ouattara NK, Passerat J, Servais P. Faecal contamination of water and sediment in the rivers of the Scheldt drainage network. Environ Monit Assess 2011;183:243–57. http://dx.doi.org/10.1007/s10661-011-1918-9.

Ouattara NK, de Brauwere A, Billen G, Servais P. Modelling faecal contamination in the Scheldt drainage network. J Mar Syst 2013. http://dx.doi.org/10.1016/j.jmarsys.2012.05.004. [in press].

Pachepsky YA, Shelton DR. *Escherichia coli* and fecal coliforms in freshwater and estuarine sediments. Crit Rev Environ Sci Technol 2011;41:1067–110. http://dx.doi.org/10.1080/10643380903392718.

Pachepsky YA, Sadeghi AM, Bradford SA, Shelton DR, Guber AK, Dao T. Transport and fate of manure-borne pathogens: modeling perspective. Agric Water Manag 2006;86:81–92. http://dx.doi.org/10.1016/j.agwat.2006.06.010.

Partheniades E. Erosion and deposition of cohesive soils. J Hydraul Div 1965;91:105–39.

Rodrigues M, Oliveira A, Guerreiro M, Fortunato A, Menaia J, David L, et al. Modeling fecal contamination in the Aljezur coastal stream (Portugal). Ocean Dyn 2011;61:841–56. http://dx.doi.org/10.1007/s10236-011-0392-9.

Romeiro NML, Castro RGS, Cirilo ER, Natti PL. Local calibration of coliforms parameters of water quality problem at Igapó I Lake, Londrina, Paraná, Brazil. Ecol Model 2011;222:1888–96. http://dx.doi.org/10.1016/j.ecolmodel.2011.03.018.

Ruelland D, Billen G, Brunstein D, Garnier J. SENEQUE: a multi-scaling GIS interface to the Riverstrahler model of the biogeochemical functioning of river systems. Sci Total Environ 2007;375:257–73. http://dx.doi.org/10.1016/j.scitotenv.2006.12.014.

Sanders BF, Arega F, Sutula M. Modeling the dry-weather tidal cycling of fecal indicator bacteria in surface waters of an intertidal wetland. Water Res 2005;39:3394–408. http://dx.doi.org/10.1016/j.watres.2005.06.004.

Schnauder I, Bockelmann-Evans B, Lin B. Modelling faecal bacteria pathways in receiving waters. Proc Inst Civ Eng Marit Eng 2007;160:143–53. http://dx.doi.org/10.1680/maen.2007.160.4.143.

Servais P, Billen G, Rego JV. Rate of bacterial mortality in aquatic environment. Appl Environ Microbiol 1985;49:1448–54.

Servais P, Billen G, Goncalves A, Garcia-Armisen T. Modelling microbiological water quality in the Seine river drainage network: past, present and future situations. Hydrol Earth Syst Sci 2007a;11:1581–92.

Servais P, Garcia-Armisen T, George I, Billen G. Fecal bacteria in the rivers of the Seine drainage network (France): sources, fate and modelling. Sci Total Environ 2007b;375:152–67. http://dx.doi.org/10.1016/j.scitotenv.2006.12.010.

Stapleton CM, Wyer MD, Kay D, Bradford M, Humphrey N, Wilkinson J, et al. Fate and transport of particles in estuaries. Numerical modelling for bathing water enterococci estimation in the Severn estuary, vol. IV. Environmental Agency Science Report SC000002/SR4; 2007.

Steets BM, Holden PA. A mechanistic model of runoff-associated fecal coliform fate and transport through a coastal lagoon. Water Res 2003;37:589–608. http://dx.doi.org/10.1016/s0043-1354(02)00312-3.

Stidson RT, Gray CA, McPhail CD. Development and use of modelling techniques for real-time bathing water quality predictions. Water Environ J 2011:7–18. http://dx.doi.org/10.1111/j.1747-6593.2011.00258.x.

Stolzenbach KD, Newman KA, Wong CS. Aggregation of fine particles at the sediment–water interface. J Geophys Res Oceans 1992;97:17889–98. http://dx.doi.org/10.1029/92jc01827.

Thieu V, Billen G, Garnier J. Nutrient transfer in three contrasting NW European watersheds: the Seine, Somme, and Scheldt Rivers. A comparative application of the Seneque/Riverstrahler model. Water Res 2009;43:1740–54. http://dx.doi.org/10.1016/j.watres.2009.01.014.

van der Wal D, van Kessel T, Eleveld MA, Vanlede J. Spatial heterogeneity in estuarine mud dynamics. Ocean Dyn 2010;60:519–33. http://dx.doi.org/10.1007/s10236-010-0271-9.

van Kessel T, Vanlede J, de Kok J. Development of a mud transport model for the Scheldt Estuary. Cont Shelf Res 2011;31:S165–81.

Vanderborght JP, Folmer IM, Aguilera DR, Uhrenholdt T, Regnier P. Reactive-transport modelling of C, N and O_2 in a river–estuarine–coastal zone system: application to the Scheldt Estuary. Mar Chem 2007;106:92–110.

Vanoni VA, editor. Sedimentation engineering, number 54 in Manuals and Reports on Engineering Practice. American Society of Civil Engineers; 2006.

Vergeynst L, Vallet B, Vanrolleghem PA. Modeling pathogen fate in stormwaters by a particle–pathogen interaction model using population balances. 6th international conference on sewer processes and networks. Australia: Surfers Paradise; 2010.

Verlaan PAJ, Donze M, Kuik P. Marine vs fluvial bottom mud in the Scheldt Estuary. Estuar Coast Shelf Sci 1998;46:873–83. http://dx.doi.org/10.1006/ecss.1999.0599.

Wu J, Rees P, Storrer S, Alderisio K, Dorner S. Fate and transport modeling of potential pathogens: the contribution from sediments. J Am Water Res Assoc 2009;45:35–44. http://dx.doi.org/10.1111/j.1752-1688.2008.00287.x.

Zhu X, Wang JD, Solo-Gabriele HM, Fleming LE. A water quality modeling study of non-point sources at recreational marine beaches. Water Res 2011;45:2985–95. http://dx.doi.org/10.1016/j.watres.2011.03.015.